

Screening effects in a density functional theory based description of molecular junctions in the Coulomb blockade regime

R. Stadler,¹ V. Geskin,² and J. Cornil²¹*Department of Physical Chemistry, University of Vienna, Sensengasse 8/7, A-1090 Vienna, Austria*²*Laboratory for Chemistry of Novel Materials, University of Mons, Place du Parc 20, B-7000 Mons, Belgium*

(Received 14 January 2009; revised manuscript received 19 February 2009; published 25 March 2009)

We recently introduced a method based on density functional theory and a nonequilibrium Green's function technique for calculating the addition energies of single-molecule nanojunctions in the Coulomb blockade regime. Here we apply this approach to benzene molecules lying parallel and at various distances from two aluminum fcc (111) surfaces, and we discuss the distance dependence in our calculations in terms of electrostatic screening effects. The addition energies near the surface are reduced by about a factor of 2, which is comparable to previously reported calculations employing a computationally far more demanding quasiparticle description.

DOI: [10.1103/PhysRevB.79.113408](https://doi.org/10.1103/PhysRevB.79.113408)

PACS number(s): 71.15.Mb, 71.10.-w

A key issue in the emerging field of molecular electronics is the description of electron transport between nanoscale contacts, for which considerable progress has been recently achieved at the experimental level.¹ Theoretically, two limiting regimes can be distinguished, namely, coherent transport (CT) for strong coupling between the molecule and the electrodes and Coulomb blockade (CB) for weak coupling. The CB regime is best described by stability diagrams, where frontiers between low- and high-conductivity domains in bias and gate voltage coordinates are reflected by diamond-like shapes.²⁻⁴ For a proper description of these diagrams, the energy difference between the ionization and affinity levels of the inserted quantum dot or single molecule (commonly referred to as addition energies E_{add}) has to be evaluated.

The first-principles nonequilibrium Green's function (NEGF) methods⁵⁻⁸ combined with density functional theory (DFT), which have been successfully used for the CT regime, are not so straightforward to apply for electron transfer under CB conditions, since an integer charge is transferred and results in a relaxation of the electronic structure of the central molecule. In principle only a many-body approach provides a general solution to the latter problem,⁹⁻¹¹ and even quasiparticle calculations based on the *GW* approximation¹² were found to not fully capture the impact of local spin and charge fluctuations in the CB regime.¹³ The suitability of a standard DFT framework for electron transport in both the CB and CT regimes was also debated^{14,15} due to the self-interaction of electrons¹⁶ in a Kohn-Sham (KS) framework and the lack of a derivative discontinuity (Ref. 17) in the evolution of KS eigenenergies.

As outlined above a main source of discrepancy with a DFT description of weakly coupled nanostructures relies on the fact that the gap between the highest occupied molecular-orbital (HOMO) and lowest unoccupied molecular-orbital (LUMO) eigenenergies in a single-particle KS scheme does not match in general the total-energy difference between the ground state and lowest charged states when the size of the HOMO-LUMO gap is finite.¹⁸ This mismatch has been recently addressed in realistic calculations of E_{add} with standard DFT techniques in three different ways. (i) For metal

particles of finite size, a modified KS gap has been introduced, where the energetic difference between the HOMO (or LUMO) for charged and uncharged clusters has been directly taken into account.¹⁹ (ii) For the description of the HOMO-LUMO gap in C₆₀-metal interfaces, the charging energy has been obtained by using a constrained DFT formalism,²⁰ where the occupation of hand-picked orbitals can be defined as a constraint in the input.²¹ (iii) Within a NEGF-DFT framework, E_{add} has been defined via threshold values of an external gate voltage V_{gate} determined via a midpoint integration rule from induced charge transfer between small molecules (H₂ and benzene) and lithium wires.²²

In this work, we adopt the approach introduced in Ref. 22 and apply it to calculate E_{add} for a benzene molecule lying parallel and at various distances from two aluminum fcc (111) surfaces (see Fig. 1). We focus in particular on the dependence of E_{add} on the distance between the central molecule and the two electrodes, and we argue that our method correctly describes screening effects that lead to a reduction in the molecular gap due to the rearrangement of the electronic structure at the Al surfaces. This is supported by two key findings. (i) the distance dependence of E_{add} (with a correction term accounting for the geometric capacitance²³) is consistent with a purely electrostatic model for screening based on image charges.²⁴ (ii) The magnitude of screening is comparable to values obtained for a variety of systems with *GW*,²⁵ constrained DFT,²⁰ and a recently developed quantum-chemical approach,²⁶ where electrodes have been

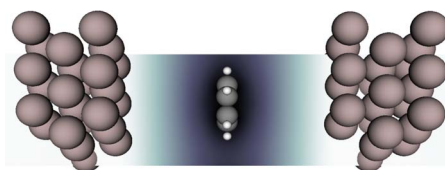


FIG. 1. (Color online) Geometry and shape of the applied gate potential for a benzene molecule lying parallel and weakly coupled to two Al fcc (111) surfaces for a distance of 8 Å. The profile of V_{gate} (taken from the differences in spatial resolution for calculations at 10 and 0 V) is shown with gray shading with its maximum located in the black regions.

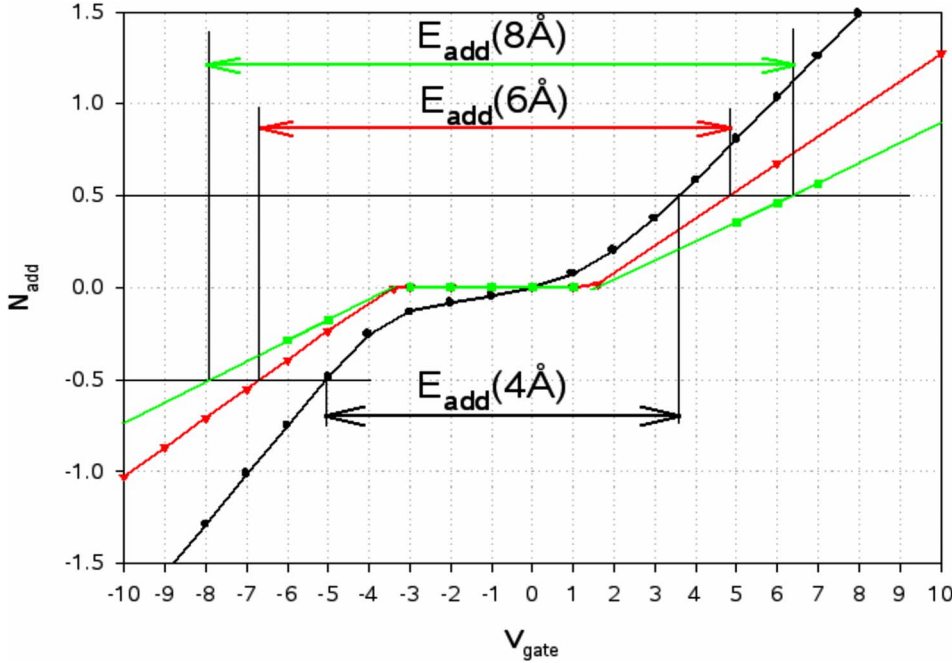


FIG. 2. (Color online) Evolution of the added/removed electrons on the benzene molecule N_{add} (obtained by spatial integration of the electron density) as a function of V_{gate} for three distances between the molecule and Al surfaces ($d_{\text{AlB}}=4, 6,$ and 8 \AA). The values of E_{add} reported elsewhere in this Brief Report are taken from such plots.

treated as a classical shape-dependent continuum, allowing to reproduce accurately the experimental data reported in Ref. 3.

Figure 1 displays the system on which we performed the NEGF-DFT calculations with the commercially available ATK software.²⁷ The scattering region contains three layers of a 3×3 unit cell of Al on each side of the benzene molecule and three additional layers on each side of the left and right electrode regions, respectively, where a 3×3 k -point grid has been used for the sampling in the transverse Brillouin plane. All atoms in the Al layers have been left in their truncated bulk positions for the experimental lattice constant of 4.05 \AA . A double-zeta polarized and single-zeta basis set have been used for the molecule and Al surfaces, respectively, and the local-density approximation (LDA) has been chosen for the exchange-correlation functional. The Keldysh formalism⁵ allows for a self-consistent solution for the electron density of the open system as a whole for every value of the external gate potential V_{gate} .²² The shape of the effective potential generated by V_{gate} is illustrated as gray shades in Fig. 1.

In Fig. 2 we illustrate how we determine the addition energy from NEGF-DFT calculations, $E_{\text{add}}^{\text{calc}}$, for varying aluminum-benzene distances d_{AlB} ,

$$\begin{aligned} E_{\text{add}}^{\text{calc}} &= \int_0^1 dN_{\text{add}} V_{\text{gate}}(N_{\text{add}}) - \int_{-1}^0 dN_{\text{add}} V_{\text{gate}}(N_{\text{add}}) \\ &= V_{\text{gate}}(N_{\text{add}} = +0.5e) - V_{\text{gate}}(N_{\text{add}} = -0.5e). \end{aligned} \quad (1)$$

We provided a formal justification for Eq. 1 in Ref. 22, where we also discussed its validity and demonstrated numerical agreement with other reliable data for H_2 and benzene molecules, respectively, attached to Li wires. The relevance of $N_{\text{add}} = \pm 0.5$ comes from the integration only; we calculate $E_{\text{add}}^{\text{calc}}$ as the energy corresponding to the integral of V_{gate} over a transferred charge of ± 1 . This energy represents

the input required for the transfer of one electron from the molecule to the two electrodes or vice versa in terms of the external potential V_{gate} inducing this transfer. We stress that this method includes screening effects implicitly, as evidenced by the fact that the results do depend on d_{AlB} (see Fig. 2).

One should keep in mind that $E_{\text{add}}^{\text{calc}}$ consists of a sum of two terms: the first related to the modified molecular HOMO-LUMO gap in the junction and the second to the electrostatic capacitance of the metallic electrodes.²⁸ The latter is usually referred to as the geometric capacitance contribution to the charging energy in the literature²³ and will be denoted as E_{geom} in the following; it can be safely neglected in the analysis of CB experiments on single-molecule junctions since it scales with d_{AlB}/A and the area of the electrodes A is usually well above tens of μm^2 , whereas the distance d_{AlB} between the molecule and the electrode surfaces is in the \AA range. This is not the case, however, in our calculations. Because we apply periodic boundary conditions to the electronic structure in the plane perpendicular to the transport direction, the finite charges are transferred from the molecule to the metal surface in each unit cell. This means that A is defined by only nine atoms in the plane and only d_{AlB} is of similar size as in the experiments, and as a consequence E_{geom} reaches the same order of magnitude than the energetic contribution from the molecular gap. In order to make our results meaningful with respect to experimental values, we define a corrected addition energy as

$$E_{\text{add}}^{\text{corr}} = E_{\text{add}}^{\text{calc}} - E_{\text{geom}} = E_{\text{add}}^{\text{calc}} - \frac{1}{2} \frac{e^2 (d_{\text{AlB}} - x_0)}{2\epsilon_0 A}, \quad (2)$$

where e denotes the elementary charge and ϵ_0 denotes the dielectric constant of vacuum. Since the system is equivalent to two capacitors in parallel, the charging energy E_{geom} contains an additional factor of $\frac{1}{2}$. Our expression for E_{geom} is

TABLE I. Corrected addition energies $E_{\text{add}}^{\text{corr}}$ for three distances d_{AIB} between the Al fcc (111) surfaces and the central benzene molecule; E_{geom} has been subtracted for a meaningful comparison with experiments. The uncorrected values $E_{\text{add}}^{\text{calc}}$ are also given in parentheses. We provide in two additional columns the corresponding data for systems with Al and Li atomic chains as electrodes in order to connect our discussion to Ref. 22. The wire lattice constants have been chosen as $a_{\text{Al}}=2.39$ and $a_{\text{Li}}=2.9$ Å and the areas of the unit cell perpendicular to the wires as $A_{\text{Al}}=4a_{\text{Al}} \times 4a_{\text{Al}}$ and $A_{\text{Li}}=3a_{\text{Li}} \times 3a_{\text{Li}}$. The position of the capacitor planes used for determining E_{geom} is taken as $x_0=2.0$ Å for both Al fcc and Al wire electrodes and $x_0=2.3$ Å for the Li wires in accordance with the differences in interlayer spacings (Ref. 29). All values for $E_{\text{add}}^{\text{corr}}$ and $E_{\text{add}}^{\text{calc}}$ are given in eV.

d_{AIB} (Å)	Al fcc (111)	Al wire	Li wire
4	7.27 (8.69)	8.26 (9.25)	8.78 (9.80)
6	8.68 (11.51)	10.18 (12.16)	9.82 (12.03)
8	10.02 (14.27)	11.19 (14.16)	10.99 (14.40)

rather approximate in the sense that it amounts to replacing the molecule by a third metallic electrode with the same area A as the source and drain electrodes. In Eq. (2) $d_{\text{AIB}}-x_0$ accounts for the difference in position between the planes of the nuclei and the electrons focal points due to spilling effects, which defines the position of the surface in any purely electrostatic (and therefore not atomistic) model and corresponds to the image plane in the model for screening we introduce below.²⁹

We collect in Table I the values for $E_{\text{add}}^{\text{corr}}$ for three different distances d_{AIB} and contrast them with calculations for the one-dimensional systems studied in Ref. 22. For the largest distance of 8 Å, the results for Li and Al wires as electrodes come rather close to the limiting case ($E_{\text{gap}}^0=11.54$ eV, as calculated from total-energy differences for charged and neutral benzene molecules²²), whereas the presence of the surface induces a gap reduction for Al fcc. A decrease in d_{AIB} reduces $E_{\text{add}}^{\text{corr}}$ for all three types of electrodes due to screening effects which are distance dependent; the HOMO-LUMO gap at 4 Å represents 63%, 72%, and 76% of E_{gap}^0 with the Al surfaces, Al wires, and Li wires, respectively. These numbers are comparable to those found for other systems.^{20,25,26} Although screening is usually associated with the interaction of charges with surfaces, a similar albeit quantitatively smaller effect can also be observed in Table I for the wire electrodes.

In order to validate the $E_{\text{add}}^{\text{corr}}(d_{\text{AIB}})$ values provided by our approach, we have also estimated the corresponding numbers from an image charge model. For that purpose we define the molecular contribution to E_{add} (the capacitive term E_{geom} does not enter the picture here, since it is a correction for the finiteness of the unit cell, whereas the image charge model assumes an infinite surface by definition) as

$$\begin{aligned} E_{\text{add}}^{\text{image}} &= [E(N+1) - E(N)] - [E(N) - E(N-1)] \\ &= E_{\text{gap}}^0 + \Sigma(N+1) + \Sigma(N-1) = E_{\text{gap}}^0 - E_{\text{screen}}, \end{aligned} \quad (3)$$

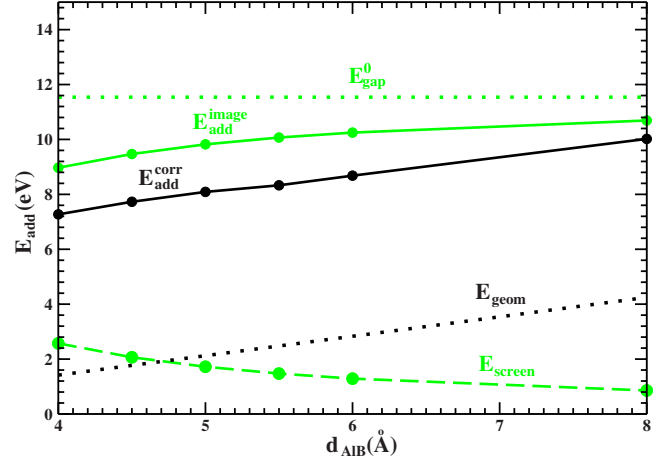


FIG. 3. (Color online) Evolution of $E_{\text{add}}^{\text{corr}}$ as a function of d_{AIB} , as extracted from NEGF-DFT calculations and compared to $E_{\text{add}}^{\text{image}}$ [for its definition see Eq. (3)]. $E_{\text{gap}}^0=11.54$ eV as calculated in Ref. 22.

with $E(N \pm 1) = E^0(N \pm 1) + \Sigma(N \pm 1)$. E_{gap}^0 denotes the difference between the electron affinity and ionization potential of the free molecule and Σ denotes the correction due to screening (i.e., the image energies associated to the charges that are calculated following the detailed recipe given in the supplementary information of Ref. 24). $\Sigma(N)=0$, since there are no screening effects when the benzene molecule is neutral, because it does not exhibit any polar bonds.

We compare in Fig. 3 the distance dependence of E_{add} as obtained from NEGF-DFT calculations via Eqs. (1) and (2) to the results provided by the image charge model, i.e., we test the assumption

$$E_{\text{add}}^{\text{image}}(d_{\text{AIB}}) \approx E_{\text{add}}^{\text{corr}}(d_{\text{AIB}}). \quad (4)$$

The deviations between $E_{\text{add}}^{\text{image}}$ and $E_{\text{add}}^{\text{corr}}$ are less than 20% of the total value of $E_{\text{add}}^{\text{corr}}$ for the range of d_{AIB} values under consideration. This is quite remarkable given the approximative nature of (i) E_{screen} [defining the d_{AIB} dependence of $E_{\text{add}}^{\text{image}}$ via Eq. (3)] since only the charge distribution inside the molecule has been described realistically by using Mulliken charges²⁴ for the larger distances or the self-consistent density on a real-space grid²² for the smallest distance and (ii) E_{geom} [contributing to $E_{\text{add}}^{\text{corr}}$ via Eq. (2)] for which the molecule and metal surfaces have been replaced by capacitor planes without taking into account any details of their atomic structures. When d_{AIB} gets smaller (close to 4 Å), it also has to be considered that wave-function overlap, which is not included in electrostatic models, starts to play a role so that the agreement between $E_{\text{add}}^{\text{image}}$ and $E_{\text{add}}^{\text{corr}}$ is expected to be better at large distances.

Finally, we want to position our work in the context of the other recently proposed methods for the theoretical description of CB experiments with single-molecule junctions. The modified KS scheme of Ref. 19 is based on finite systems and therefore not directly suitable to study screening effects. Our method differs from those in Refs. 25 and 26 by its level of accuracy; although inferior to a full quasiparticle description,²⁵ which can treat only rather small systems, our approach is preferable to a semiempirical method,²⁶ where

the predictive power is limited by the need to find suitable parameters. The technique in Ref. 20 based on constrained DFT²¹ is rather close to our approach in the sense that it also enforces the occupation of molecular orbitals and calculates E_{add} from the energy required to uphold this charging. However, while we apply an external gate voltage V_{gate} , let the electron density relax as a function of it and determine E_{add} from the threshold values for V_{gate} , the occupation of the HOMO/LUMO is fixed manually in Ref. 20, thus introducing a certain amount of arbitrariness (at least for not so weakly coupled systems), and the key quantity is the gradient of orbital eigenenergy with its occupation. We stress that all these methods find a gap reduction due to screening effects by about a factor of 2, in good agreement with our results.

In summary, we have extended a recently introduced method for the calculation of addition energies E_{add} for single-molecule junctions in the CB regime²² by describing in a more realistic way the electrode surfaces. This paves the

way toward NEGF-DFT-based predictions of E_{add} for junctions characterized in recent experimental studies,³ where screening effects are likely to play a major role. We analyzed the distance dependence of E_{add} in comparison to an image charge model and to other techniques developed for determining E_{add} and found an overall good agreement among all approaches, suggesting a reduction in the electronic gap by up to 50% in molecular junctions.

This research has been supported by the European Commission with the projects SINGLE (FP7/2007-2013) (Grant No. 213609) and MODECOM (Grant No. NMP3-CT-2006-016434), the Interuniversity Attraction Pole Program of the Belgian Federal Science Policy Office (PAI 6/27), and the Belgian National Fund for Scientific Research (FNRS). We are especially indebted to J. A. Torres for his advice. J.C. in particular is funded by the FNRS. R.S. is currently supported by the Austrian Science Fund FWF (Project No. P20267).

-
- ¹*Introducing Molecular Electronics*, Lecture Notes in Physics Vol. 680, edited by G. Cuniberti, G. Fagas, and K. Richter (Springer, New York, 2005).
- ²L. P. Kouwenhoven, D. G. Austing, and S. Tarucha, *Rep. Prog. Phys.* **64**, 701 (2001).
- ³S. Kubatkin, A. Danilov, M. Hjort, J. Cornil, J. L. Bredas, N. Stuhr-Hansen, P. Hedegård, and T. Bjørnholm, *Nature (London)* **425**, 698 (2003); A. Danilov, S. Kubatkin, S. Kafanov, P. Hedegård, N. Stuhr-Hansen, K. Moth-Poulsen, and T. Bjørnholm, *Nano Lett.* **8**, 1 (2008).
- ⁴A. Nitzan and A. Ratner, *Science* **300**, 1384 (2003).
- ⁵M. Brandbyge, J. L. Mozos, P. Ordejon, J. Taylor, and K. Stokbro, *Phys. Rev. B* **65**, 165401 (2002).
- ⁶Y. Xue, S. Datta, and M. A. Ratner, *Chem. Phys.* **281**, 151 (2002).
- ⁷A. R. Rocha, V. M. Garcia-Suarez, S. W. Baily, C. J. Lambert, J. Ferrer, and S. Sanvito, *Nature Mater.* **4**, 335 (2005).
- ⁸K. S. Thygesen and K. W. Jacobsen, *Chem. Phys.* **319**, 111 (2005).
- ⁹P. Delaney and J. C. Greer, *Phys. Rev. Lett.* **93**, 036805 (2004).
- ¹⁰S. Datta, arXiv:cond-mat/0603034 (unpublished); B. Muralidharan, A. W. Ghosh, and S. Datta, *Phys. Rev. B* **73**, 155410 (2006); *Mol. Simul.* **32**, 751 (2006).
- ¹¹S. M. Lindsay and M. A. Ratner, *Adv. Mater. (Weinheim, Ger.)* **19**, 23 (2007).
- ¹²K. S. Thygesen and A. Rubio, *Phys. Rev. B* **77**, 115333 (2008).
- ¹³X. Wang, C. D. Spataru, M. S. Hybertsen, and A. J. Millis, *Phys. Rev. B* **77**, 045119 (2008).
- ¹⁴C. Toher, A. Filippetti, S. Sanvito, and K. Burke, *Phys. Rev. Lett.* **95**, 146402 (2005).
- ¹⁵M. Koentopp, C. Chang, K. Burke, and R. Car, *J. Phys.: Condens. Matter* **20**, 083203 (2008).
- ¹⁶J. P. Perdew and A. Zunger, *Phys. Rev. B* **23**, 5048 (1981).
- ¹⁷J. P. Perdew, R. G. Parr, M. Levy, and J. L. Balduz, *Phys. Rev. Lett.* **49**, 1691 (1982).
- ¹⁸W. Kohn, *Phys. Rev. B* **33**, 4331(R) (1986).
- ¹⁹K. Capelle, M. Borgh, K. Kärkkäinen, and S. M. Reimann, *Phys. Rev. Lett.* **99**, 010402 (2007).
- ²⁰J. D. Sau, J. B. Neaton, H. J. Choi, S. G. Louie, and M. L. Cohen, *Phys. Rev. Lett.* **101**, 026804 (2008).
- ²¹Q. Wu and T. Van Voorhis, *Phys. Rev. A* **72**, 024502 (2005).
- ²²R. Stadler, V. Geskin, and J. Cornil, *Phys. Rev. B* **78**, 113402 (2008).
- ²³M. Büttiker, *J. Phys.: Condens. Matter* **5**, 9361 (1993); A. Sakai, S. Kurokawa, and Y. Hasegawa, *J. Vac. Sci. Technol. A* **14**, 1219 (1996); S. Kurokawa and A. Sakai, *J. Appl. Phys.* **83**, 7416 (1998); J. Wang, H. Guo, J. L. Mozos, C. C. Wan, G. Taraschi, and Q. Zheng, *Phys. Rev. Lett.* **80**, 4277 (1998).
- ²⁴D. J. Mowbray, G. Jones, and K. S. Thygesen, *J. Chem. Phys.* **128**, 111103 (2008).
- ²⁵J. B. Neaton, M. S. Hybertsen, and S. G. Louie, *Phys. Rev. Lett.* **97**, 216405 (2006).
- ²⁶K. Kaasbjerg and K. Flensberg, *Nano Lett.* **8**, 3809 (2008).
- ²⁷ATK, Version 2.2, atomistix a/s, 2004, www.atomistix.com
- ²⁸J. M. Thijssen and H. S. J. Van der Zant, *Phys. Status Solidi B* **245**, 1455 (2008).
- ²⁹N. D. Lang and W. Kohn, *Phys. Rev. B* **7**, 3541 (1973).